Preprints of the 19th World Congress
The International Federation of Automatic Control
Cape Town, South Africa. August 24-29, 2014

Full-State Autopilot-Guidance Design Under a Linear Quadratic Differential Game Formulation

Maital Levy, Tal Shima, and Shaul Gutman

Technion - Israel Institute of Technology, 32000 Haifa Israel
(E-Mails: maital@tx.technion.ac.il, tal.shima@technion.ac.il, and mergutm@technion.ac.il)

Abstract: Full-state single-loop and full-state two-loop autopilot-guidance designs are derived using a linear quadratic differential game formulation. To keep all the states at reasonable values throughout the end-game, a cost function that includes appropriate running cost terms on some of the states is proposed. It is proven that the two designs may be identical under a linear quadratic differential game formulation and the proposed cost function. The theorem and guidance laws are illustrated using an interceptor missile having forward and aft controls.

1. INTRODUCTION

The term full-state guidance law refers to an autopilot-guidance system that has a full-state feedback into the guidance loop. This may enhance the interceptor homing performance by accounting for the coupling between the control and guidance dynamics. In a previous paper (Levy et al. [2013]), two types of full-state autopilot-guidance schemes were considered - single-loop and two-loop schemes. In the two-loop case, the inner autopilot loop is designed separately from the outer guidance loop, whereas in the single-loop scheme, the guidance commands are issued directly to the actuators, without a definite autopilot. It was proven under a linear quadratic formulation that the two full-state schemes achieve the same performance if and only if the number of guidance commands is identical to the number of available controllers.

In previous papers, full-state G&C systems were denoted as "integrated" guidance systems. In Palumbo et al. [2004], Shima et al. [2006], Idan et al. [2007], Menon and Ohlmeyer [2001], Menon et al. [2003], Park et al. [2011], the term "integrated" referred to a single-loop guidance system, where there is not a definite autopilot component. In a previous paper Shkolnikov et al. [2001], a two-loop autopilot-guidance system is designed, where the term "integrated" referred to the full-state feedback into the guidance law. In Rusnak and Levi [1991] the general solution of an optimal guidance law with a full-state feedback was derived for an arbitrary order autopilot model.

The controller deflection of practical missiles is bounded, thus a nonlinear system has to be treated during saturation. In fact, during saturation the G&C loop is opened and if in addition the open loop transfer function is unstable or close to instability, the attitude angle may diverge to unacceptable values. In the nonlinear approach, the states can be kept at reasonable values by placing a limitation on the commands and using a carefully designed autopilot. Using the linear quadratic approach, this can be done indirectly by adding appropriate running state cost terms.

Perfect information of the target future maneuver is usually not available. Hence, an appropriate alternative to the optimal control formulation is the zero-sum pursuit-evasion game formulation (Isaacs [1965]), where only the information on the target maneuver capability is required. A linear quadratic differential game (LQDG) formulation was presented in Ho et al. [1965] while assuming ideal dynamics for both adversaries. In Ben-Asher and Yaesh [1998], this assumption was replaced by first-order dynamics for both the missile and the target. In Shima and Golan [2007] an LQDG-type guidance law was derived for a dual controlled missile, where the pursuer dynamics was approximated by two first-order bi-proper transfer functions

In this paper, it is shown that under an LQDG formulation and running state cost terms, the two full-state schemes (single-loop and two-loop) are identical if and only if the number of guidance commands is identical to the number of available controllers. The guidance laws performance is studied using two types of target maneuver: LQDG and a "Bang-Bang". The miss distance sensitivity to adding running cost terms is analysed.

The remainder of this paper is organized as follows. The problem formulation and the full-state autopilot-guidance schemes and theorem are presented in sections 2 and 3, respectively. The test case is given in section 4 and the simulation results are provided in section 5. Section 6 presents the concluding remarks.

2. PROBLEM FORMULATION

This section provides the design assumptions and describes the linearized endgame geometry used for the synthesis of the guidance laws and their analysis.

2.1 Design Assumptions

The derivation of the guidance laws will be performed based on the following assumptions:

(1) A skid-to-turn roll-stabilized missile is considered. The motion of such a missile can be separated into two perpendicular channels, thus allowing to treat only a planar motion.
(2) Both the evading target and the pursuing missile have linear dynamics.
(3) The missile and target deviations from the collision triangle are small during the end-game. In this manner, the relative end-game trajectory can be linearized about the nominal line of sight (LOS).
(4) Constant speeds are assumed for both the missile and the target.

2.2 End-Game Scenario Description

Fig. 1 presents a schematic view of the planar endgame geometry, where X axis is aligned with the initial LOS (LOS_0) and Z axis is perpendicular to it. The subscripts P and E denote the pursuing missile and the evading target, respectively. V, a, and γ denote the speed, normal acceleration, and path angle. a_{PN}, and a_{EN} are respectively the pursuer and evader accelerations normal to LOS_0. r is the range between the adversaries and λ is the angle between the LOS and the X axis. y is the relative displacement between the target and the missile normal to the X axis.

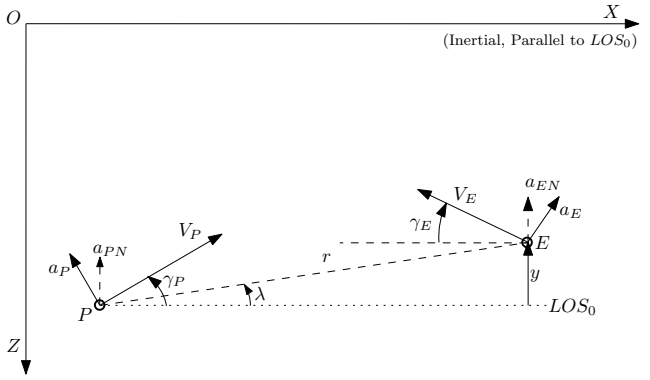

Fig. 1. Planar Engagement Geometry

The pursuer and evader accelerations normal to the initial line of sight are

$$a_{PN} \approx a_P cos(\gamma_{P0}), \quad a_{EN} \approx a_E cos(\gamma_{E0}) \tag{1}$$

Then, the corresponding kinematic equation is

$$\ddot{y} = a_{EN} - a_{PN} \tag{2}$$

2.3 Linear Equations of Motion

The general set of equations can be classified into three categories:

(1) Kinematics (guidance) equations [1], $\mathbf{x_G} \in \mathcal{R}^{n_G \times 1}$
(2) Dynamics equations, $\mathbf{x_D} \in \mathcal{R}^{n_D \times 1}$
(3) Servo model equations [2] , $\mathbf{x_S} \in \mathcal{R}^{n_S \times 1}$

[1] $\mathbf{x_G}$ contains the kinematical states of the engagement, e.g. the missile-target separation and separation rate etc.
[2] The equations of motion take into account the servo dynamics.

The target dynamics is assumed to be ideal to consider a realistic scenario where there is no information on its dynamics. In this manner, by assuming ideal target dynamics, the worst-case scenario is taken into account. Let $v \in \mathcal{R}^1$ denote the target controller, then

$$a_{EN} = v \tag{3}$$

The dynamics and servo equations of the missile are given as follows

$$\begin{bmatrix} \dot{\mathbf{x}}_\mathbf{D} \\ \hline \dot{\mathbf{x}}_\mathbf{S} \end{bmatrix} = \left[\begin{array}{c|c} \mathbf{A_{DD}} & \mathbf{A_{DS}} \\ \hline [\mathbf{0}] & \mathbf{A_S} \end{array}\right] \begin{bmatrix} \mathbf{x_D} \\ \hline \mathbf{x_S} \end{bmatrix} + \begin{bmatrix} [\mathbf{0}] \\ \hline \mathbf{B_S} \end{bmatrix} \tilde{\mathbf{u}} \tag{4}$$

where $\tilde{\mathbf{u}} \in \mathcal{R}^{m \times 1}$ is the input to the missile servo. Note that $\mathbf{u} \in \mathcal{R}^{m_G \times 1}$ will denote the guidance controller.

The set of kinematic equations is given by

$$\dot{\mathbf{x}}_\mathbf{G} = \left[\, \mathbf{A_{GG}} \,|\, \mathbf{A_{G,DS}} \,\right] \begin{bmatrix} \mathbf{x_G} \\ \hline \mathbf{x_D} \\ \mathbf{x_S} \end{bmatrix} + \mathbf{C_G} v \tag{5}$$

Finally, the general set of equations is given by

$$\dot{\mathbf{x}} = \mathbf{A}\mathbf{x} + \mathbf{B}\tilde{\mathbf{u}} + \mathbf{C}v, \quad \mathbf{x} = \left[\mathbf{x_G^T}\ \mathbf{x_D^T}\ \mathbf{x_S^T}\right]^\mathbf{T} \tag{6}$$

where

$$\begin{aligned} \mathbf{A} &= \left[\begin{array}{c|c} \mathbf{A_{GG}} & \mathbf{A_{G,DS}} \\ \hline \begin{matrix}[\mathbf{0}] \\ [\mathbf{0}]\end{matrix} & \begin{matrix}\mathbf{A_{DD}} & \mathbf{A_{DS}} \\ [\mathbf{0}] & \mathbf{A_S}\end{matrix} \end{array}\right] \\ \mathbf{B} &= \begin{bmatrix} [\mathbf{0}] \\ \hline [\mathbf{0}] \\ \mathbf{B_S} \end{bmatrix}, \quad \mathbf{C} = \begin{bmatrix} \mathbf{C_G} \\ \hline [\mathbf{0}] \\ [\mathbf{0}] \end{bmatrix} \end{aligned} \tag{7}$$

The general form of Eq. (6) is time varying. For simplicity of presentation, the time dependency is not explicitly written.

In its general form, the measurement equation of the pursuer normal acceleration can be expressed as

$$a_{PN} = \mathbf{H}\mathbf{x} \tag{8}$$

Using Eq. (2), the kinematics state space formulation is given by

$$\begin{aligned} \mathbf{x_G} &= [y\ \dot{y}]^T \\ \mathbf{A_{GG}} &= \begin{bmatrix} 0 & 1 \\ 0 & 0 \end{bmatrix}, \mathbf{A_{G,DS}} = \begin{bmatrix} \mathbf{0} \\ -\mathbf{H} \end{bmatrix}, \mathbf{C_G} = \begin{bmatrix} 0 \\ 1 \end{bmatrix} \end{aligned} \tag{9}$$

3. FULL-STATE AUTOPILOT-GUIDANCE DESIGN UNDER AN LQDG FORMULATION

In this section, the full-state single-loop and two-loop guidance laws are provided. Then, a theorem concerned with the condition for achieving the same performance for both guidance laws is presented.

3.1 Full-State Single-Loop

The full-state single-loop optimization problem is described in Fig. 2 and given in Eqs. (10-11).

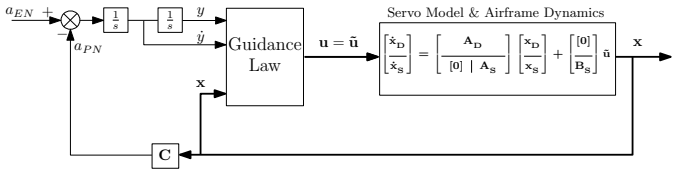

Fig. 2. Full-State Single-Loop Scheme

$$J = \mathbf{x}^T(t_f)\mathbf{Q_f}\mathbf{x}(t_f) + \int_{t_0}^{t_f} \left(\mathbf{u}^T\mathbf{R}\mathbf{u} + \mathbf{x}^T\mathbf{Q}\mathbf{x} - Ev^2\right) d\tau \tag{10}$$

$$\dot{\mathbf{x}} = \mathbf{A_{1L}}\mathbf{x} + \mathbf{B_{1L}}\tilde{\mathbf{u}} + \mathbf{C}v, \quad \mathbf{A_{1L}} = \mathbf{A}, \quad \mathbf{B_{1L}} = \mathbf{B} \tag{11}$$

$$\mathbf{u} = \tilde{\mathbf{u}}, \quad \mathbf{x} = \left[\mathbf{x_G^T}\ \mathbf{x_D^T}\ \mathbf{x_S^T}\right]^{\mathbf{T}} \tag{12}$$

where, the matrices $\mathbf{A}$, $\mathbf{B}$ and $\mathbf{C}$ are given in Eq. (7). The subscript $1L$ denotes the single-loop configuration. The target guidance command v is given by an LQDG guidance law or any other scalar law (constant, step etc).

3.2 Full-State Two-Loop

The full-state two-loop optimization problem is presented in Fig. 3 and given in Eqs. (3) and (13-14).

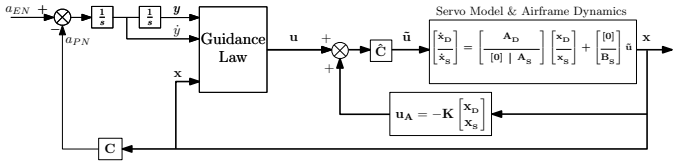

Fig. 3. Full-State Two-Loop Scheme

$$\begin{aligned} J &= \mathbf{x}^T(t_f)\mathbf{Q_f}\mathbf{x}(t_f) + \int_t^{t_f} (\tilde{\mathbf{u}}^{\mathbf{T}}\tilde{\mathbf{R}}\tilde{\mathbf{u}} + \mathbf{x}^T\mathbf{Q}\mathbf{x} - Ev^2)d\tau = \\ &= \mathbf{x}^T(t_f)\mathbf{Q_f}\mathbf{x}(t_f) + \\ &\int_t^{t_f} \left(\mathbf{u}^{\mathbf{T}}\mathbf{R_A}\mathbf{u} + \mathbf{2x}^{\mathbf{T}}\mathbf{S_A}\mathbf{u} + \mathbf{x}^{\mathbf{T}}(\mathbf{Q_A} + \mathbf{Q})\mathbf{x} - Ev^2\right) d\tau \end{aligned} \tag{13}$$

$$\dot{\mathbf{x}} = \mathbf{A_{2L}}\mathbf{x} + \mathbf{B_{2L}}\mathbf{u} + \mathbf{C}v, \quad \mathbf{x} = \left[\mathbf{x_G^T}\ \mathbf{x_D^T}\ \mathbf{x_S^T}\right]^{\mathbf{T}} \tag{14}$$

where the subscript $2L$ denotes the two-loop configuration and

$$\mathbf{A_{2L}} = \left[\begin{array}{c|c} \mathbf{A_{GG}} & \mathbf{A_{G,DS}} \\ \hline \begin{matrix}\mathbf{[0]}\\ \mathbf{[0]}\end{matrix} & \begin{matrix}\mathbf{A_{DD}} & \mathbf{A_{DS}} \\ -\mathbf{B_S}\hat{\mathbf{C}}\mathbf{k_D} & \mathbf{A_S} - \mathbf{B_S}\hat{\mathbf{C}}\mathbf{k_S}\end{matrix} \end{array}\right], \quad \mathbf{B_{2L}} = \begin{bmatrix}\mathbf{[0]}\\ \mathbf{B_S}\hat{\mathbf{C}}\end{bmatrix} \tag{15}$$

$$\mathbf{Q_A} = \left[\begin{array}{c|c} \begin{matrix}\mathbf{[0]} & \mathbf{[0]}\end{matrix} \\ \hline \begin{matrix}\mathbf{[0]} & \hat{\mathbf{Q}}\end{matrix} \end{array}\right], \quad \mathbf{S_A} = \left[\begin{array}{c} \mathbf{[0]} \\ \hline \hat{\mathbf{S}} \end{array}\right], \quad \mathbf{R_A} = \hat{\mathbf{R}} = \hat{\mathbf{C}}^{\mathbf{T}}\hat{\mathbf{C}}$$

$$\hat{\mathbf{Q}} = \begin{bmatrix}\mathbf{k_D^T}\hat{\mathbf{C}}^{\mathbf{T}}\hat{\mathbf{C}}\mathbf{k_D} & \mathbf{k_D^T}\hat{\mathbf{C}}^{\mathbf{T}}\hat{\mathbf{C}}\mathbf{k_S} \\ \mathbf{k_S^T}\hat{\mathbf{C}}^{\mathbf{T}}\hat{\mathbf{C}}\mathbf{k_D} & \mathbf{k_S^T}\hat{\mathbf{C}}^{\mathbf{T}}\hat{\mathbf{C}}\mathbf{k_S}\end{bmatrix}, \quad \hat{\mathbf{S}} = \begin{bmatrix}-\mathbf{k_D^T} \\ -\mathbf{k_S^T}\end{bmatrix}\hat{\mathbf{C}}^{\mathbf{T}}\hat{\mathbf{C}} \tag{16}$$

3.3 Full-State Guidance Laws Theorem

The theorem is formulated for the general form of the full-state guidance laws under an LQDG formulation.

Theorem 1. The necessary and sufficient condition for obtaining identical solutions to the optimization problems of the full-state single-loop case (6-7,13) and of the full-state two-loop case (13-15) is that $\hat{\mathbf{C}}$ is nonsingular.

Proof. Following the details of the proof given in Levy et al. [2013], Theorem 1 can be easily proven, since the target control effort and running state cost terms are identical for both the single-loop and two-loop cases.

4. TEST CASE

The chosen test case is a dual-controlled exo-atmospheric missile where a nose jet device was added to a thrust vector control (TVC) missile (see Levy et al. [2013] for additional details).

$$\begin{bmatrix}\dot{\mathbf{x}}_\mathbf{D}\\ \hline \dot{\mathbf{x}}_\mathbf{S}\end{bmatrix} = \left[\begin{array}{c} \mathbf{A_D} \\ \hline \mathbf{[0]}\,|\,\mathbf{A_S} \end{array}\right]\begin{bmatrix}\mathbf{x_D}\\ \hline \mathbf{x_S}\end{bmatrix} + \begin{bmatrix}\mathbf{[0]}\\ \hline \mathbf{B_S}\end{bmatrix}\tilde{\mathbf{u}} \tag{17}$$

where the states are

$$\mathbf{x_D} = \left[\theta\ \dot{\theta}\right]^{\mathbf{T}}, \quad \mathbf{x_S} = \left[\delta_n\ \delta_t\right]^{\mathbf{T}}, \quad \tilde{\mathbf{u}} = \left[\delta_{n_c}\ \delta_{t_c}\right]^{\mathbf{T}} \tag{18}$$

and the model matrices are given by

$$\begin{aligned} \mathbf{A_D} &= \begin{bmatrix}0 & 1 & 0 & 0\\ 0 & 0 & M_{\delta_n} & -M_{\delta_t}\end{bmatrix}, \quad \mathbf{A_S} = \begin{bmatrix}-1/\tau_n & 0\\ 0 & -1/\tau_t\end{bmatrix} \\ \mathbf{B_S} &= \begin{bmatrix}1/\tau_n & 0\\ 0 & 1/\tau_t\end{bmatrix} \end{aligned} \tag{19}$$

The measurement equation is given by

$$a_{PN} = \frac{T}{m}\begin{bmatrix}1 & 0 & 1 & 1\end{bmatrix}\begin{bmatrix}\mathbf{x_D}\\ \mathbf{x_S}\end{bmatrix} \tag{20}$$

Two types of autopilot block diagrams are considered (see Levy et al. [2013] for additional details). Figs. 4-5 present the single-input and multi-input autopilot diagrams, respectively. It can be seen that different servo commands are issued in each case. In the single-input case, the guidance law command is scalar, whereas in the multi-input case there are two guidance commands that match the number of available controllers.

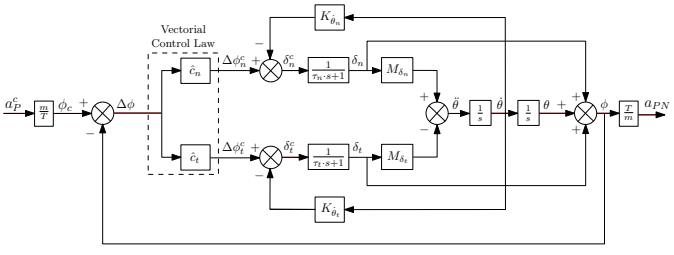

Fig. 4. Single-Input Autopilot Block Diagram

5. RESULTS

In this section, the full-state two-loop autopilot-guidance law is compared to the full-state single-loop guidance law. Simulations were made for two types of target acceleration commands: (1)LQDG guidance law (2)"Bang-bang"

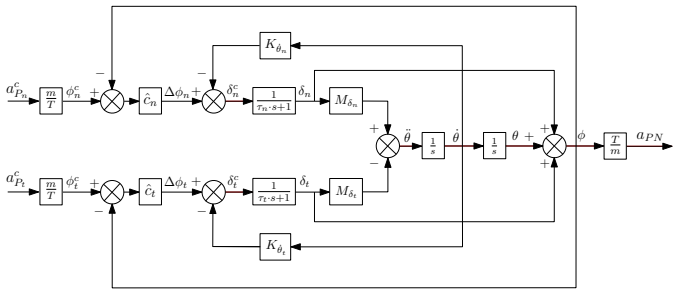

Fig. 5. Multi-Input Autopilot Block Diagram

controller. The latter is the optimal evasive strategy subject to a bounded target command (Gutman and Goldan [2009], Shinar and Steinberg [1977]). Table 1 presents the scenario parameters, where V_{max} denotes the maximum target acceleration.

Parameter	Value	Units
τ_n, τ_t	0.1	sec
T/m	200	m/sec^2
V_{max}	15	m/sec^2
y_0	50	m
M_{δ_n}, M_{δ_t}	330	$1/sec^2$

Table 1. Scenario Parameters Values

5.1 LQDG Target Maneuver

In this case, both adversaries use an LQDG guidance law. The cost function of the single-loop case is given by

$$J = a^2 y^2(t_f) + \int_{t_0}^{t_f} \{\alpha^2 {\delta_n^c}^2 + \delta_t^{c2} - \rho^2 v^2\} d\tau \qquad (21)$$

Figs. 6-7 present the results of the full-state single-loop and full-state two-loop guidance laws for the penalties: a =2, α = 1, ρ = 0.5. It can be seen that the results of the single-loop case and two-loop case with a multi-input autopilot overlap. In this case, the target hardly maneuvers, since the LQDG guidance command is proportional to the entire state vector including y. Thus, the LQDG guidance law is not suitable to represent a realistic evading strategy. It is evident that θ is kept within its physical domain, thus a running cost term was not required (see Eq. (21)).

The concept of the Pareto curve will be used to compare the performance of the full-state single-loop and the full-state two-loop schemes (see Levy et al. [2013] for additional information). The Pareto curve in Fig. 8 was created by changing the weight α for a fixed a weight that practically guarantees zero miss distance. It can be seen that the curves of the full-state single-loop and of the full-state two-loop with a multi-input autopilot overlap, thus implying they achieved the same performance. The Pareto curve of the two-loop case with a single-input autopilot is significantly higher than the one obtained in the full-state single-loop one. When a single-input autopilot is used, the guidance command does not have the sufficient degrees of freedom (two) to issue the appropriate command to each of the controllers.

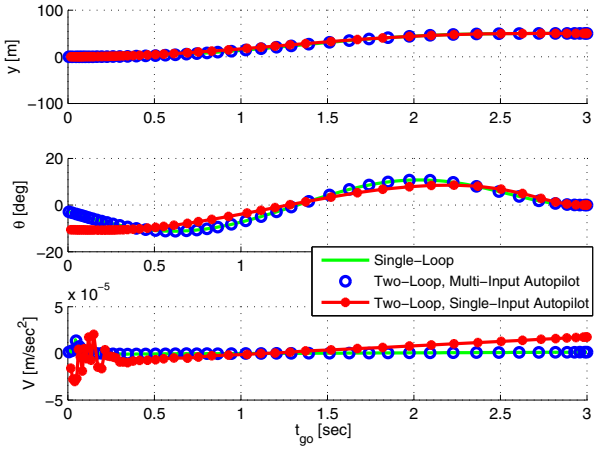

Fig. 6. y and θ and the Target Acceleration Command (LQDG Target Maneuver, a =2, α = 1, ρ = 0.5)

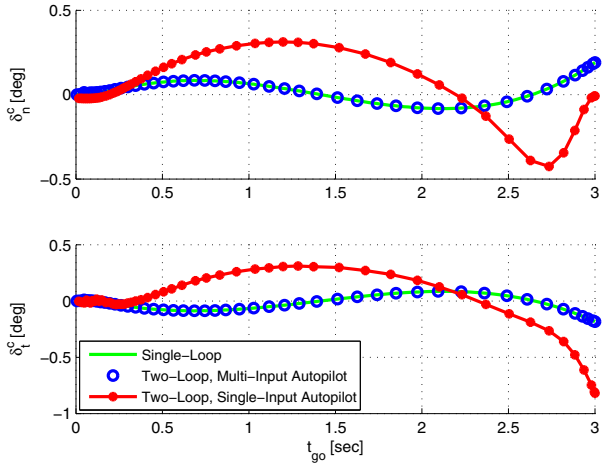

Fig. 7. Servo Commands (LQDG Target Maneuver, a =2, α = 1, ρ = 0.5)

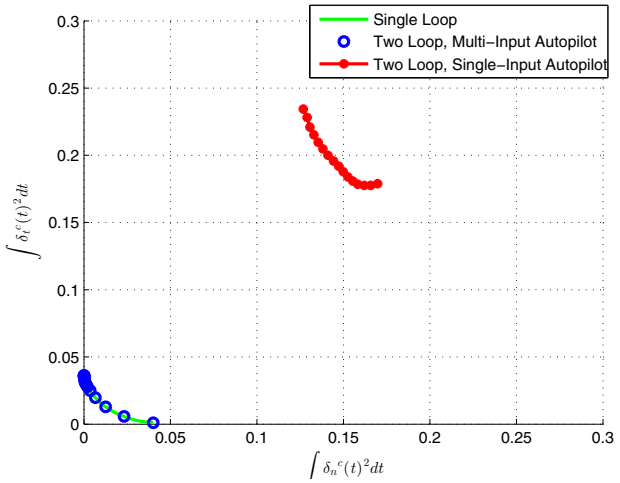

Fig. 8. Pareto Front Curves for a Perfect Interception case (LQDG Target Maneuver, a = 2, ρ = 0.5)

5.2 "Bang-Bang" Target Maneuver

In this case, the target has a "bang-bang" type evasive strategy with a known acceleration limit, V_{max}. Fig. 9 presents the typical target maneuver that is considered in this case.

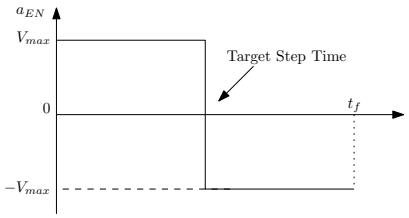

Fig. 9. Target Maneuver - "Bang Bang"

In the previous section, the angle θ did not exceed beyond its physical domain due to the small target commands. In this case, it will be seen that appropriate running cost terms must be added to the cost function to keep θ at reasonable values.

Fig. 10 presents the maximum value of θ and the miss distance for different target step times without a running cost term on θ. It can be seen that the value of $|\theta|_{max}$ exceeds beyond its physical domain for most step time values. When a single-input autopilot diagram is used, both controllers are always active, thus the obtained tail deflection is larger than the deflection in the multi-input autopilot case. As a result, there is larger pitch down moment and θ is decreased. It can be seen that the miss distance of the two-loop case with a single-input is higher than the miss distance of the single-loop case. The latter, implies the superiority of the single-loop and two-loop with a multi-input autopilot over the two-loop with a single-input autopilot. As a result, the following analysis design will be done for the single-loop case [3].

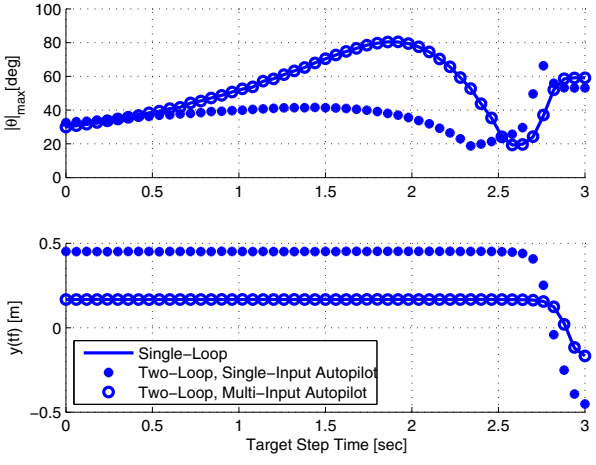

Fig. 10. $|\theta|$ versus Target Step Time ("Bang-Bang" Target Maneuver, $a = 0.3$, $\alpha = 1$, $\rho = 0.1$)

In order to keep the attitude angle at acceptable values, the full-state single-loop design will be designed subject to the following cost function

[3] The analysis can be equally done on the two-loop multi-input autopilot case.

$$J = a^2 y^2(t_f) + \int_{t_0}^{t_f} \{\alpha^2 \delta_n^{c\,2} + \delta_t^{c2} + q^2\theta^2 - \rho^2 v^2\} d\tau \quad (22)$$

The weight q will be designed for the target step time that achieved the possible maximum θ. In this way, θ will be kept at reasonable values for the possible target step times. The maximum, $\theta \sim 80.4^0$ is obtained when the target performs an acceleration step command at 1.86 [sec].

Figs. 11-12 present the simulation results of a full-state single-loop guidance law with a target step command at 1.86 [sec]. It can be seen that by adding an appropriate running cost term to the cost function, θ maintained reasonable values, where $\theta_{max} \sim 24.5^0$. The obtained miss distance is still acceptable (0.17 [m] for q=0 and 0.18 [m] for q=0.25).

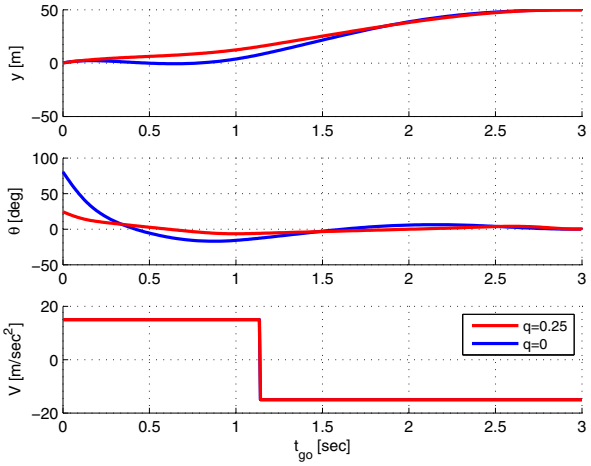

Fig. 11. y and θ and the Target Acceleration Command ("Bang-Bang" Target Maneuver, $a = 0.3$, $\alpha = 1$, $\rho = 0.1$, $q = 0$)

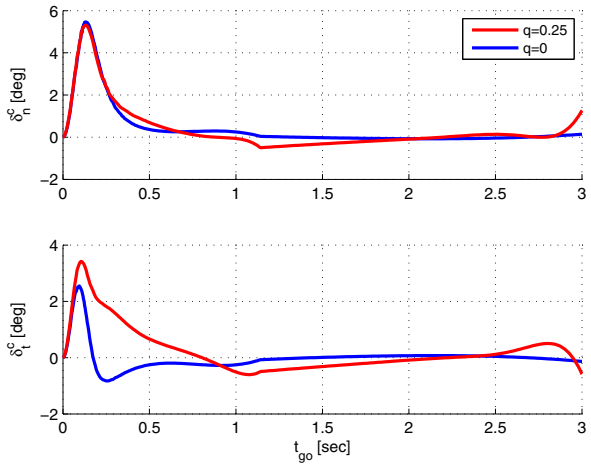

Fig. 12. Servo Commands ("Bang-Bang" Target Maneuver, $a = 0.3$, $\alpha = 1$, $\rho = 0.1$)

Fig. 13 presents the value of maximum value of θ and the miss distance for different values as a function of the target step time. It can be seen that by taking $q = 0.25$, the values of θ and the miss distance were kept at reasonable values for all the possible target step times.

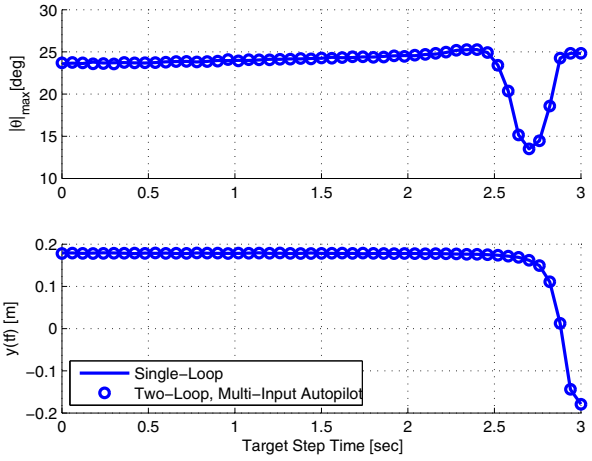

Fig. 13. $|\theta|$ versus Target Step Time ("Bang-Bang" Target Maneuver, $a = 0.3$, $\alpha = 1$, $\rho = 0.1$, q =0.25)

6. CONCLUSIONS

In this paper, full-state single-loop and two-loop autopilot-guidance schemes were explored under a linear quadratic differential game formulation. It was proven that the two full-state guidance law are identical if and only if the number of guidance commands matches to the number of available controllers.

Simulation results have shown that by the attitude angle may be kept at reasonable values by proper penalization, while still obtaining the required miss distance.

REFERENCES

J. Z. Ben-Asher and I. Yaesh. *Advances in Missile Guidance Theory*, volume 180. American Institute of Aeronautics and Astronautics, Reston, Virginia, 1998. pp. 25–88.

S. Gutman and O. Goldan. Proportional navigation miss distance in the presence of bounded inputs. *AIAA Journal of Guidance, Control, and Dynamics*, 35(3): 816–823, 2009. doi: 10.2514/1.41713.

Y.-C. Ho, A. Bryson, and S. Baron. Differential games and optimal pursuit-evasion strategies. *Automatic Control, IEEE Transactions on*, 10(4):385–389, 1965. doi: 10.1109/TAC.1965.1098197.

M. Idan, T. Shima, and O. M. Golan. Integrated sliding mode autopilot-guidance for dual-control missiles. *AIAA Journal of Guidance, Control, and Dynamics*, 30 (4):1081–1089, 2007. doi:10.2514/1.24953.

R. Isaacs. *Differential games: a mathematical theory with applications to warfare and pursuit, control and optimization*. Wiley, New York, 1965.

M. Levy, T. Shima, and S. Gutman. Single vs. two-loop full-state multi-input multi-output missile guidance. In *Proceedings of the AIAA Guidance, Navigation, and Control Conference*, Boston, Massachusetts, 2013.

P. K. Menon and E. J. Ohlmeyer. Integrated design of agile missile guidance and autopilot systems. *Control Engineering Practice*, 9(10):1095–1106, 2001. doi:10.1016/S0967-0661(01)00082-X.

P. K. Menon, G. D. Sweriduk, and E. J. Ohlmeyer. Optimal fixed-interval integrated guidance-control laws for hit-to-kill missiles. In *AIAA Guidance, Navigation, and Control Conference*, pages 1–9, 11-14 Aug 2003.

N. F. Palumbo, B. E. Reardon, and R. A. Blauwkamp. Integrated guidance and control for homing missiles. *Johns Hopkins Apl Technical Digest*, 25(2):121–139, 2004.

B.-G. Park, T.-H. Kim, and M.-J. Tahk. Time-delay control for integrated missile guidance and control. *International Journal of Aeronautical and Space Science*, 12(3):260–265, 2011. doi:10.5139/IJASS.2011.12.3.260.

I. Rusnak and M. Levi. Modern guidance law for high-order autopilot. *AIAA Journal of Guidance, Control, and Dynamics*, 14(5):1056–1058, 1991. doi: 10.2514/3.20749.

T. Shima and O. M. Golan. Linear quadratic differential games guidance law for dual controlled missiles. *IEEE Transactions on Control Systems Technology*, 43(3): 834–842, 2007. doi:10.1109/TAES.2007.4383577.

T. Shima, M. Idan, and O. M. Golan. Sliding–mode control for integrated missile autopilot guidance. *AIAA Journal of Guidance, Control, and Dynamics*, 29(2):250–260, 2006. doi:10.2514/1.14951.

J. Shinar and D. Steinberg. Analysis of optimal evasive maneuvers based on a linearized two-dimensional kinematic model. *Journal of Aircraft*, 14(8):795–802, 1977. doi: 10.2514/3.58855.

I. Shkolnikov, Y. B. Shtessel, and D. Lianos. Integrated guidance-control system of a homing interceptor: Sliding mode approach. In *Proceeding of the AIAA Guidance, Navigation, and Control Conference*, pages 1–11, August 6–9 2001. doi:10.2514/6.2001-4218.